Biocatalysis and Agricultural Biotechnology 22 (2019) 101372

Contents lists available at ScienceDirect

Biocatalysis and Agricultural Biotechnology

journal homepage: http://www.elsevier.com/locate/bab

Cloning, expression and characterization of a novel (2R,3R) -2,3-butanediol dehydrogenase from *Bacillus thuringiensis*

Feng-Qin Gong [a,b,1], Qi-Shun Liu [a,1], Hai-Dong Tan [a], Tang Li [a], Cheng-Yu Tan [b], Heng Yin [a,*]

[a] Natural Products and Glyco-Biotechnology Research Group, Liaoning Provincial Key Laboratory of Carbohydrates, Dalian Institute of Chemical Physics, Chinese Academy of Sciences, CAS, Dalian, 116023, China
[b] College of Marine and Environmental Sciences, Dalian Ocean University, Dalian, 116023, China

ARTICLE INFO

Keywords:
Acetoin
Butanediol dehydrogenase
Bacillus thuringiensis

ABSTRACT

Acetoin (3-hydroxy-2-butanone) is an important four-carbon compound widely used in the food industry and other industrial applications. This study aimed to identify a novel butanediol dehydrogenase that can efficiently catalyze the formation of acetoin. A novel butanediol dehydrogenase, *Bt*BDH, was identified from *Bacillus thuringiensis* subsp. Kurstaki ACCC 10066, and its enzymatic properties were characterized. The optimum pH and temperature for the oxidation activity of *Bt*BDH were 10.0 and 50 °C, respectively, and those for the reduction activities were 7.5 and 35 °C, respectively. In addition, it exhibits stability over a wide pH range (6–10) and temperatures up to 70 °C. *Bt*BDH showed good stability after storage for 3 months at 4 °C. Moreover, ethylenediaminetetracetic acid (EDTA) inhibits the enzymatic activity of *Bt*BDH, indicating that the enzyme is metal-dependent. This study characterized a novel (2R,3R) −2,3-butanediol dehydrogenase. Its excellent oxidation activity and stability ensure its great industrial application potential in the production of acetoin.

1. Introduction

Acetoin (3-hydroxy-2-butanone) is an important four-carbon compound with a unique butter flavor and is widely used as a food flavor enhancer in the food industry (Kochius et al., 2014; Xiao and Lu, 2014). It is listed as one of the top 30 building block chemicals with the highest priority to their development and utilization by the U.S. Department of Energy (Xie et al. 2017a, 2017b). Due to its remarkable versatility, the demand for acetoin has increased in recent years, and the development of efficient production methods has attracted extensive attention.

2,3-butanediol dehydrogenase (BDH) is a widespread oxidoreductase which has been identified in different microorganisms such as *Klebsiella pneumoniae*, *Serratia marcescens* and *Enterobacter*. This enzyme is essential for catalytic synthesis of acetoin in microbial metabolic pathways. Although the upgrade of high-throughput genome sequencing has identified fairly new potential BDHs in the form of putative open reading frame, only a few have been identified as true (2R,3R) −2,3-BDH (Çelik and Aktaş, 2013; Muschallik et al., 2017). In addition, a BDH encoding gene was identified in the gram-positive bacterium *Bacillus thuringiensis*. However, to date, there have been no reports on the purification and characterization of BDH from *B. thuringiensis*.

In the present work, a novel butanediol dehydrogenase from *B. thuringiensis* subsp. Kurstaki ACCC 10066 (*Bt*BDH) was cloned, expressed, purified and characterized. It exhibits a preference for (2R,3R) −2,3-butanediol and meso-2,3-butanediol, and its activity was regulated by Zn^{2+}. To the best of our knowledge, this is the first report describing a true (2R,3R) −2,3-butanediol dehydrogenase from *B. thuringiensis*. The enzyme characterized in this study has great potential for the producing of pure acetoin.

2. Materials and methods

2.1. Materials

B. thuringiensis subsp. *Kurstaki* (ACCC 10066) was obtained from

Abbreviations: BDH, 2,3-butanediol dehydrogenase; *Bt*BDH, 2,3-butanediol dehydrogenase from *B. thuringiensis* subsp. *Kurstaki* ACCC 10066; EDTA, Ethylenediaminetetraacetic acid; IPTG, Isopropylthiogalactoside; DTT DL, Dithiothreitol; DMSO, Dimethyl sulfoxide; NaCl, Sodium chloride; SDS-PAGE, Sodium dodecyl sulfate-polyacrylamide gel electrophoresis; KDa, Kilo Dalton.

* Corresponding author.
E-mail address: yinheng@dicp.ac.cn (H. Yin).
[1] These authors contributed equally.

https://doi.org/10.1016/j.bcab.2019.101372
Received 25 May 2019; Received in revised form 17 September 2019; Accepted 2 October 2019
Available online 3 October 2019
1878-8181/

Agricultural Culture Collection of China (Zhang et al., 2015). Plasmid pET-21a (+), *Escherichia coli* competent cell strains TOP10 and BL21 (DE3), and PCR reaction reagents were purchased from Takara Biotechnology (Dalian, China). (2R,3R) −2,3-butanediol (≥96.0%) was from Shanghai Aladdin bio-chem technology Company LTD (Shanghai, China). Meso-2,3-butanediol was purchased from sigma Ltd (Shanghai, China). (2S,3S) −2,3-butanediol (≥97.0%) was obtained from Tokyo Chemical Industry(Shanghai, China). Unless stated otherwise, all chemicals were of analytical grade.

2.2. Cloning of the butanediol dehydrogenase

Protein sequence homology analysis of *Bt*BDH (GenBank accession number WP_030023136) was performed by using Basic Local Alignment Search Tool (BLAST, http://blast.ncbi.nlm.nih.gov/Blast.cgi). The DNA sequence of *Bt*BDH was amplified from the genome of *Bacillus thuringiensis* via PCR (Polymerase Chain Reaction) using a forward primer 5′-CGCGCATATGAAAGCACTACTTTGGCAT-3′ bearing an *Nde*I restriction site (underlined) and a reverse primer 5′-CGCCCTCGAGTTATTTAGGTGAAACAAG-3′ with an *Xho*I restriction site (underlined). The PCR product was ligated into the *Nde*I-*Xho*I sites of the pET-21a (+) and then transformed into competent *E. coli* BL21 (DE3).

2.3. Expression and purification of recombinant protein

E. coli (DE3) cells were incubated in 100 ml of LB medium supplied with 0.1 mg/ml of ampicillin at 37 °C. When the OD_{600} nm reached 0.6, 0.01 mM IPTG was added and the culture was further incubated at 16 °C for 20 h. The cultured cells were harvested from the medium by centrifugation and disrupted by sonication in 20 mM Tris/HCl buffer (pH 7.4) containing 50 mM NaCl. Cell debris and unbroken cells were separated by centrifugation, and then the sample was applied to a Q Sepharose® Fast Flow column (100 × 16 mm) pre-equilibrated with 20 mM Tris/HCl buffers (pH 7.4) on a fast protein liquid chromatography system. The bound protein was eluted with the same buffer containing a linear gradient of NaCl (0–500 mM) with a flow speed of 5 mL/min. The collected active fractions were pooled and the sample buffer was changed to 20 mM Tris/HCl (pH 7.4) using Amicon ultra (EMD Millipore, USA) through repeat dilution and concentration. All purification performances were carried out at 4 °C unless otherwise stated. The purity and molecular weight of the obtained samples were determined by SDS-polyacrylamide gel electrophoresis.

2.4. Determination of protein concentration and enzyme activity

The protein concentration was determined by the BCA method (Smith et al., 1985) using bovine serum albumin as a standard. Enzyme activities were determined spectrophotometrically by measuring the absorption at 340 nm which is corresponding to the formation of NAD (H). Oxidation activities were performed in 50 mM glycin/NaOH buffer (pH 10.0) with 1 mM NAD^+ as the cofactor, while the reduction activities were measured in 50 mM sodium phosphates (pH 7.5) with 0.3 mM NADH as the cofactor. One unit (U) of *Bt*BDH activity was defined as the amount of enzyme that oxidized or reduced one μmol of NADH or NAD^+, respectively, per minute under the given conditions.

2.5. Optimal pH and stability

The optimal pH of *Bt*BDH activity were determined at 4 °C by using diacetyl, racemic acetoin or (2R,3R) −2,3-butanediol (10 mM each) as substrates and NAD^+ (1 mM) or NADH (0.3 mM) as corresponding cofactors. The reactions were carried out at different pH values, including 50 mM acetate buffer (pH 3.0–5.8), 50 mM sodium phosphate buffer (pH 7.0–8.0), Tris/HCl buffer (pH 7.0–8.0) and 50 mM glycine/NaOH buffer (pH 9.0–10.0), and last for 24 h. All reactions were performed in triplicates and the relative activity was calculated.

2.6. Optimal temperature and thermo stability

To explore the optimal temperatures of *Bt*BDH, the oxidative activity of the enzyme was determined in 50 mM sodium glycine buffer (pH 10.0), and the reductive activity of the enzyme was performed in 50 mM PBS (pH 7.5). All reactions were carried out at temperatures within the range of 20 °C–80 °C. For the thermo stability of *Bt*BDH, the purified enzyme was pre-incubated at different temperatures (20 °C, 30 °C, 40 °C, 50 °C, 60 °C, 70 °C and 80 °C) for 0.5 h. The residue activity was measured and the relative activity was calculated.

2.7. Effects of metal ions and inhibitors on BtBDH activity

The enzyme was pre-incubated with different metal ion (NaCl, $CoCl_2$, $MgCl_2$, Ni_2SO_4, LiCl, $CaCl_2$, $MnCl_2$, $MnSO_4$, $ZnCl_2$, and $FeCl_3$) at a final concentration of 1 mM in 4 °C for 0.5 h, and the remained enzyme activity was measured and the relative activity was calculated. Similarly, the effects of inhibitors (DTT, EDTA, DMSO, Triton X-100, SDS, Tween 80) on enzyme activity were determined by pre-incubating the enzyme with 10.0 mM of different inhibitors for 30 min at 4 °C, and the residual activity was then measured. The residue activity was expressed as a percentage relative to the activity of control (no treatment with a metal ion or inhibitor).

2.8. Kinetic parameters

Kinetic parameters were determined under standard conditions with substrate concentrations in the range of 0–10 mM for acetoin and diacetyl; 0–100 mM for (2R,3R) −2,3-butanediol, meso-2,3-butanediol and (2S,3S) −2,3-butanediol; 0–0.5 mM for NADH and 0–0.5 mM for NAD^+. Kinetic parameters calculation was performed using GraphPad Prism version5 for Windows (GraphPad Software, La Jolla, CA, USA).

3. Result and discussion

3.1. Cloning and analysis of BtBDH

The putative *Bt*BDH (GenBank accession number WP_030023136) gene was 1053 bp long, encoding a peptide of 350 amino acids (37.8 kDa). The isoelectric point of the enzyme was calculated to be 5.5 using the website sever (https://web.expasy.org/compute_pi/). Blastp analysis against the Protein Data Bank (PDB) revealed homology of BtBDH to several dehydrogenases such as the L-Threonine dehydrogenase (TDH) from *Pyrococcus horikoshii* (PDB:2DFV, 40% identity) (Ishikawa et al., 2007), the NADP(H)-dependent ketose reductase from *Bemisia argentifolii* (PDB:1E3J, 34% identity) (Banfield et al., 2001), TDH from *Thermococcus kodakaraensis* (PDB:3GFB, 39% identity) (Bowyer et al., 2009), a uncharacterized zinc-type alcohol dehydrogenase from *Escherichia coli* (PDB:5VM2, 34% identity), and a sheep liver sorbitol dehydrogenase (PDB:3QE3, 32% identity) (Yennawar et al., 2011). Secondary structure alignment of BtBDH with these five dehydrogenases using ESPript 3.0 sever (Robert and Gouet, 2014) was showed in Fig. 1. The results revealed that *Bt*BDH has a similar amino acids distribution in the catalytic Zn site (Cys37, His69 and Glu151) and the structural Zn site (Cys99, Cys102, Cys105 and Cys113) (Gonzalez et al., 2000; Banfield et al., 2001). It also has the consensus pattern GHEXXGXXXXX(GA)XX(IVAC) found in the superfamily of the zinc-containing medium-chain alcohol dehydrogenase (MDR) (Gonzalez et al., 2000). Moreover, *Bt*BDH contains a GroES-like domain at the N terminus and a NAD(P) -binding domain at the C-terminus. Phylogenetic tree analysis revealed that *Bt*BDH is a member of (2R,3R) −2,3-BDH (Fig. 2). The analysis results show that *Bt*BDH has the typical (2R,3R) −2,3-butanediol dehydrogenase property and belongs to the MDR superfamily.

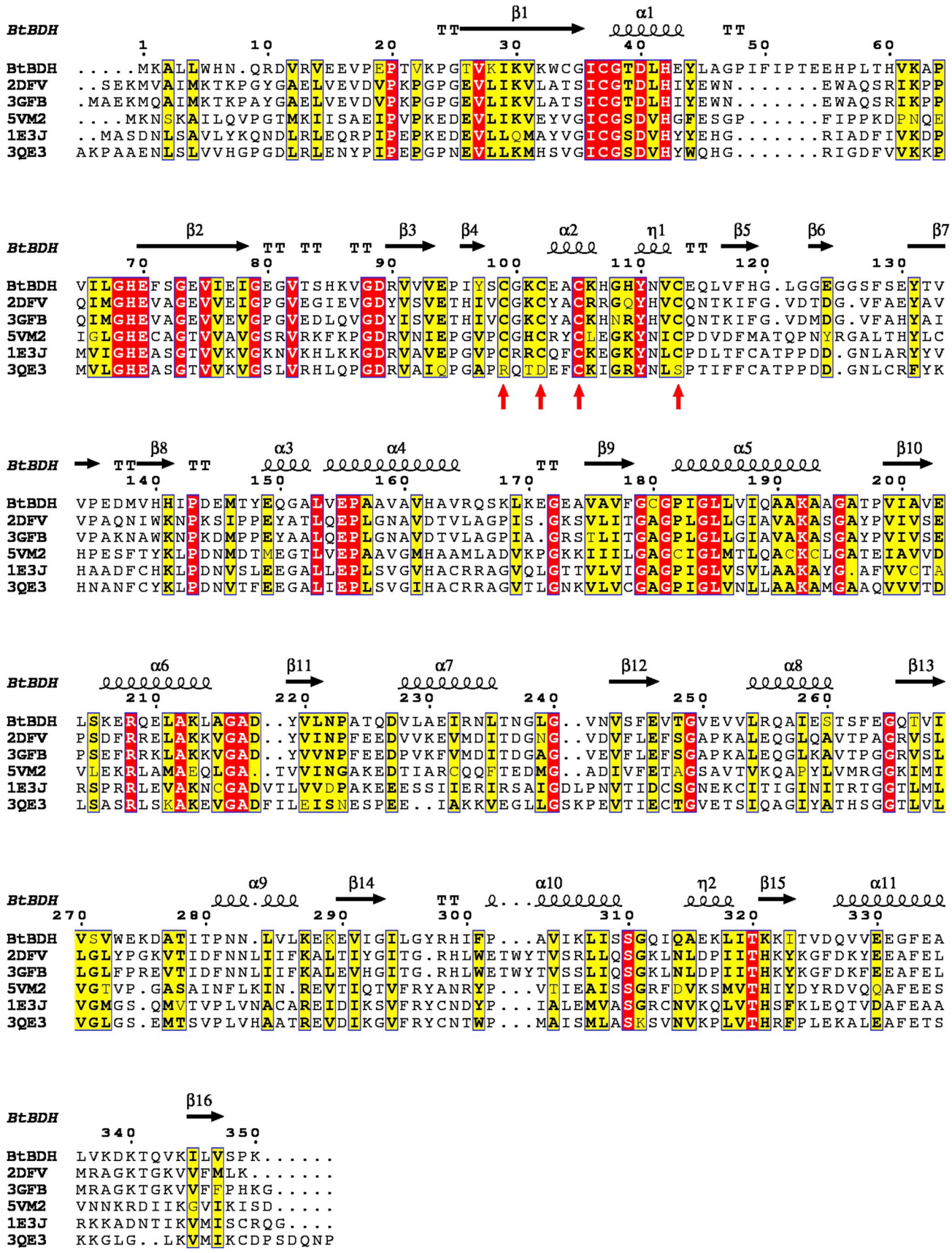

Fig. 1. Secondary structure alignment of *Bt*BDH with the five dehydrogenases. L-Threonine dehydrogenase (TDH) from *Pyrococcus horikoshii* (PDB:2DFV), NADP(H)-dependent ketose reductase from *Bemisia argentifolii* (PDB:1E3J), TDH from *Thermococcus kodakaraensis* (PDB:3GFB), a uncharacterized zinc-type alcohol dehydrogenase from *Escherichia coli* (PDB:5VM2), and a sheep liver sorbitol dehydrogenase (PDB:3QE3).

3.2. Protein expression, purification, and kinetic properties

Hydrophobic analysis using the ExPaSy Protscale program indicated that *Bt*BDH is a soluble protein. The recombinant *Bt*BDH was purified by ion exchange chromatograph. SDS-PAGE (Fig. 3 Line 3) showed a signal band with a molecular weight of approximately 40 kDa, which is consistent with the theoretical molecular weight of *Bt*BDH (37.8 kDa).

Enzymatic assay using meso-2,3-butanediol, (2R,3R) −2,3-butanediol and (2S,3S) −2,3-butanediol as substrates showed that it has BDH activity toward meso-2,3-butanediol and (2R,3R) −2,3-butanediol, whereas no activity was observed for (2S,3S) −2,3-butanediol (Table 1). Further analysis demonstrated that *Bt*BDH showed similar oxidative activity toward meso-2,3-butanediol (v_{max} = 45.25 U/mg) and (2R,3R) −2,3-butanediol (v_{max} = 43.85 U/mg), and it exhibited relatively higher reduction activity toward acetoin (37.04 U/mg) than diacetyl (13.49 U/mg). According to previous reports, (2R,3R) −2,3-BDH generally belongs to the MDR family (Gao et al., 2013; Yu et al., 2015; Muschallik et al., 2017), while meso-2,3-BDH is commonly clustered in the SDR (short chain dehydrogenase/reductase) family (Zhang et al., 2012; Xu et al., 2016). Although the amino acid sequences of (2R,3R) −2,3-BDH and meso-2,3-BDH do not belong to the same family, the crystal structure of BDHs exhibits a similar overall structure to that of meso-2,3-BDH (Otagiri et al. 2001, 2010). Furthermore, the residues responsible for NAD^+ binding are highly conserved in (2R,3R) −2,3-BDH and meso-2,3-BDH (Otagiri et al., 2010). This may be the reason that (2R,3R) −2,3-BDH can catalyze meso-2,3-butanediol and (2R,3R) −2,3-butanediol. (Celinska and Grajek, 2009; Gao et al., 2013).

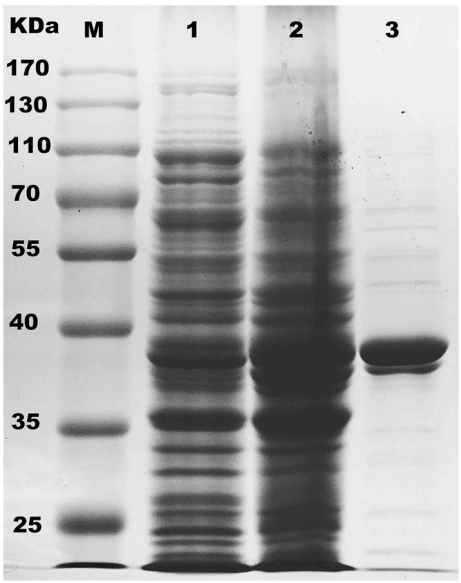

Fig. 3. SDS-PAGE analysis of expressed and purified *Bt*BDH. The proteins were separated on a 12% polyacrylamide gel and stained with Coomassie Brilliant Blue R-250. Lane M, protein size marker; lane 1, protein expressed by *E. coli* prior to IPTG induction; lane 2, crude enzyme induced by IPTG; and lane 3, purified protein.

3.3. Effects of pH and stability on enzyme activity

The effect of pH on the purified enzyme is shown in Fig. 4. The optimal pH for the oxidation and reduction activities of *Bt*BDH is 10 and 7.5, respectively (Fig. 4A), which is different from the optimum pH of 2,3-BDH from *Saccharomyces cereisiae* (Gonzalez et al., 2001) and *Clostridium ljungdahlii* (Tan et al., 2015). For most dehydrogenases in the MDR family, the optimal pH range for reduction is 6–8, and the optimal

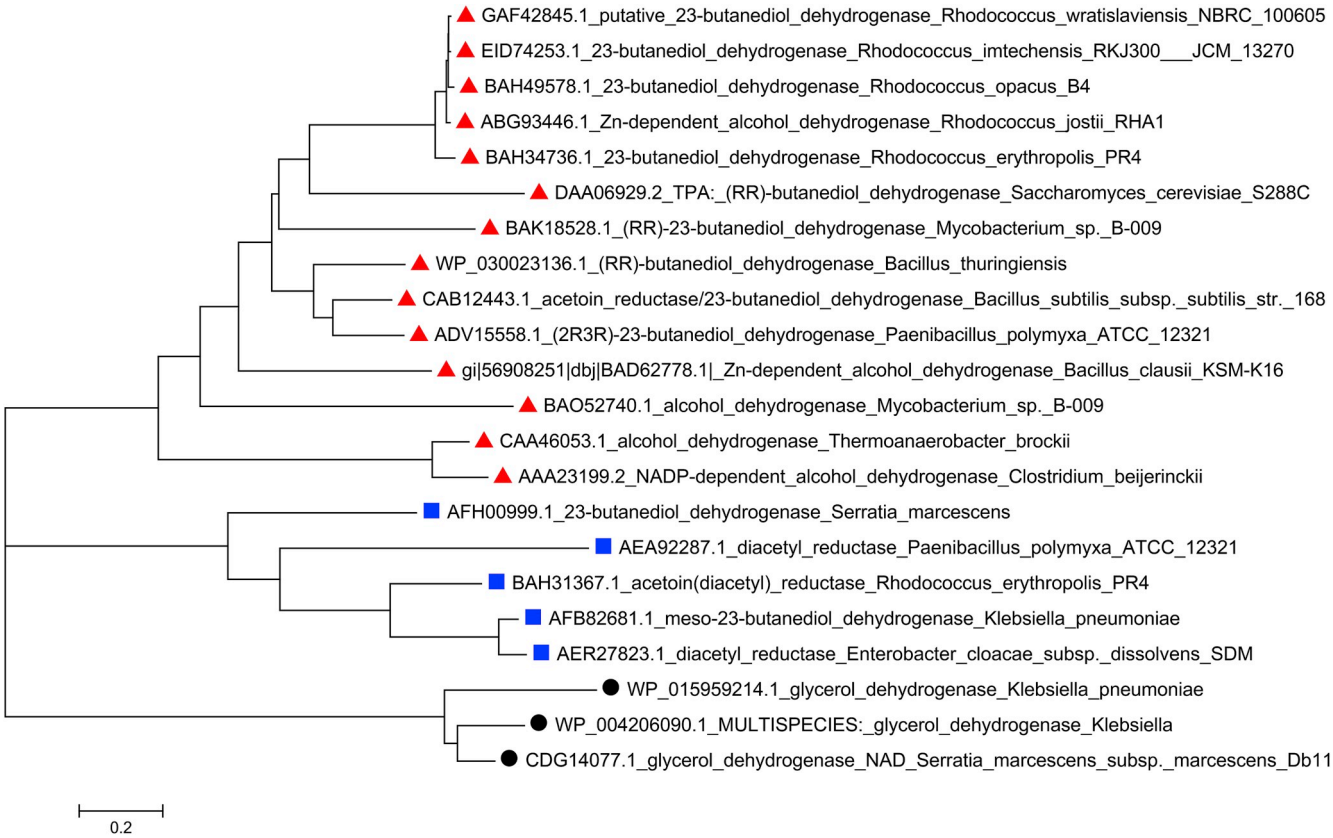

Fig. 2. The phylogenetic tree analysis of (2R,3R) −2,3-BDH from *B. thuringiensis* subsp. Square is represented by (2R,3R) −2,3-BDH, rhombohedral means glycerol dehydrogenase, and triangle means meso-2,3-BDH.

Table 1
Kinetic constants of (2R,3R) −2,3-butanediol dehydrogenase.

Substrate	Vmax [U/mg]	Km [mM]
(2R,3R) −2,3-butanediol	35.45 ± 1.40	0.76 ± 0.12
meso-2,3-butanediol	45.16 ± 1.74	3.67 ± 0.55
(2S, 3S)- 2,3- butanediol	–	–
Acetoin	36.37 ± 3.45	0.49 ± 0.08
Diacetyl	14.99 ± 1.09	0.66 ± 0.06
NAD^+	11.22 ± 0.73	0.14 ± 0.02
NADH	28.77 ± 2.02	0.23 ± 0.02

-, Activity undetectable. Values given are average of three replications. Data are the mean ± SD.

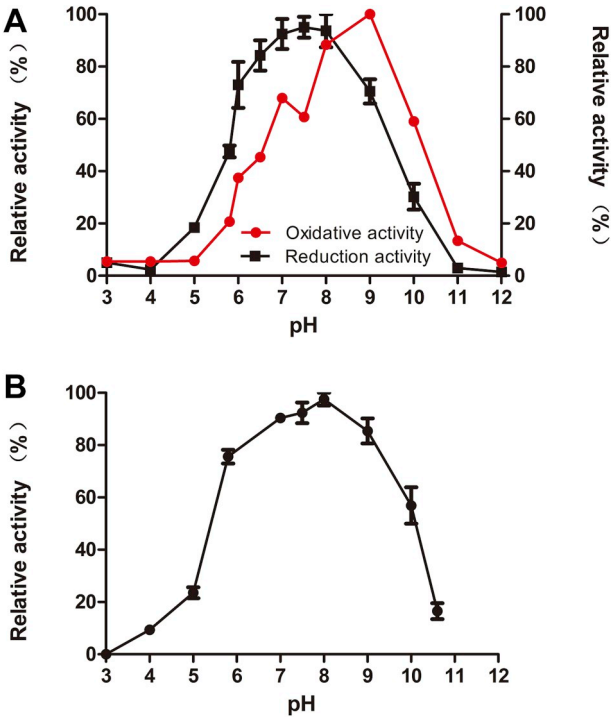

Fig. 4. Effects of pH on the *Bt*BDH activity and stability. **A** The optimal pH of *Bt*BDH activity. The reaction was carried out at different pH values, including 50 mM acetate buffer (pH 3.0–5.8), 50 mM sodium phosphate buffer (pH 7.0–8.0) or Tris/HCl buffer (pH 7.0–8.0) and 50 mM glycin/NaOH buffer (pH 9.0–10.0) **B** The pH stability of *Bt*BDH for oxidation of (2R,3R) −2,3-butanediol. The purified of *Bt*BDH in different buffers was treated for 24 h without any substrate. Data are represented in the means of triplicate experiments, and error bars are shown by the standard deviation.

pH range for oxidation is 8–11 (Gonzalez et al., 2000; Yu et al., 2015; Muschallik et al., 2017). However, for short-chain dehydrogenases, the optimal pH for reduction is within the range of 4–8 (Zhao et al., 2015). The results of *Bt*BDH indicated that when alcohol was used as substrate, the enzyme is more inclined to an alkaline environment, which is consistent with the oxidation reaction characteristics of the dehydrogenase (Raedts et al., 2014). Furthermore, the enzyme displayed remarkable pH stability ranging from 7 to 9, with residual activity remaining above 85% after 24 h incubation at 4 °C (Fig. 4B). This is in contrast to the previously reported BDHs from *Bacillus clausii* DSM 8716T (Muschallik et al., 2017), *R. erythropolis* (Yu et al., 2011) and *P. polymyxa* (Hohn-Bentz and Radler, 1978), where lower stability are observed.

3.4. Effects of temperature on the stability and activity of BtBDH

The oxidative and reductive properties of *Bt*BDH were measured using NAD(H) as a cofactor. The effects of temperature and thermal stability of *Bt*BDH are shown in Fig. 5. The optimal oxidation and reduction temperatures for the enzyme were 50 °C and 35 °C, respectively (Fig. 5A). The different optimal temperature of *Bt*BDH toward various substrates indicates its complicated catalytic mechanism. The versatile optimal temperature of the enzyme makes it suitable for different purposes, similar to other orthologous enzymes from other mesophiles microbes, which are reported to have an optimal temperature of 30 °C and 60 °C (Yu et al., 2015; Xu et al., 2016; Muschallik et al., 2017).

The thermal stability assessment of *Bt*BDH revealed that the enzyme has considerable stability up to 60 °C and retained 50% of maximum activity after 1 h incubation at 80 °C (Fig. 5B). The purified enzyme has considerable higher thermal stability than BDH from *Corynebacterium crenatum* SYPA5-5, which is very unstable when the temperature is above 35 °C (Zhao et al., 2015). *Bt*BDH was stable at 4 °C for 3 months in 20 mM Tris/HCl buffer (pH 7.4). The stability may be due to the presence of disulfide bond, which enhances the stability of the local region, thereby improving the overall stability of the enzyme. Studies have shown that disulfide bonds can reduce entropy changes in protein structure changes (significantly increase protein stability through multiple disulfide bonds).

3.5. Effects of metal ions and inhibitors on enzyme activity

The effects of metal ions and inhibitors on *Bt*BDH activity are shown in Table 2. Based on homologous modeling structure analysis (Fig. 1), *Bt*BDH belongs to the zinc-containing alcohol dehydrogenases family, in which zinc plays a vital role in structural organization, functional regulation and conformational stabilization of the protein, and ultimately activates or inactivates the enzyme (Suganya et al., 2014). Some studies have reported that zinc-containing medium-chain alcohol dehydrogenases from *Rhodococcus erythropolis* WZ010 (Yu et al., 2015), *T. guaymasensis* (Ying and Ma, 2011), *Yokenella* sp. strain WZY002 (Ying et al., 2014), *Bacillus thuringiensis serovar israelensis* (Çelik and Aktaş, 2013) (*Bt*ADH), *Acinetobacter* sp. Strain M-1 (Tani et al., 2000) and *Acinetobacter baylyi* ADP1 (Uthoff and Steinbuchel, 2012) were inhibited by exogenous zinc ions. In the present study, the activity of *Bt*BDH was promoted by a low concentration of Zn^{2+} (0.1 mM), while inhibited (86% residue activity) when the concentration of zinc increased to 10 mM (Table 3). Furthermore, remarkable stimulations of the enzyme activity were observed in the presence of K^+ and Mn^{2+}, whereas Mg^{2+}, Ca^{2+}, Co^{2+}, and Fe^{3+} have no significant effect on the activity of *Bt*BDH. In addition, cationic Ni^{2+} inhibited *Bt*BDH activity (71 ± 2.85%) (Table 2), this inhibitory effect may involve in Cysteine residues (Fig. 1) since this amino acid prone to the binding of metal ions, such as zinc, nickel and copper (Thirumoorthy et al., 2007). Unlike *Bt*BDH, *Bt*ADH (Çelik and Aktaş, 2013) is dramatically inhibited by divalent cations such as Mn^{2+}, Mg^{2+}, Ca^{2+}, Co^{2+}, and Ni^{2+} (20% residue activity), while Ba^{2+} increases the activity by 20%.

As a metalloenzyme, EDTA strongly inhibits the activity of the *Bt*BDH. Besides, the results showed that the nonionic detergent Triton X-100 and Tween 80 had no significant effect on enzyme activity. DMSO had no significant effect on *Bt*BDH activity, indicating that the enzyme has excellent organic solvents tolerance. In contrast, ionic detergent (SDS) greatly inhibited the activity of the enzyme, indicating the enzyme is sensitive to ionic detergents. Although *Bt*BDH contains 3 pairs of disulfide bonds, its activity is not inhibited by 10 mM DTT. This may be because the disulfide bonds buried in the protein molecule have large steric hindrance, hindering the access of reducing agent.

4. Conclusion

In the present study, a novel (2R,3R) −2,3-BDH from *B. thuringiensis* was successfully cloned, expressed and characterized. The maximum oxidation activity was observed at pH 10.0 and 50 °C. The maximum

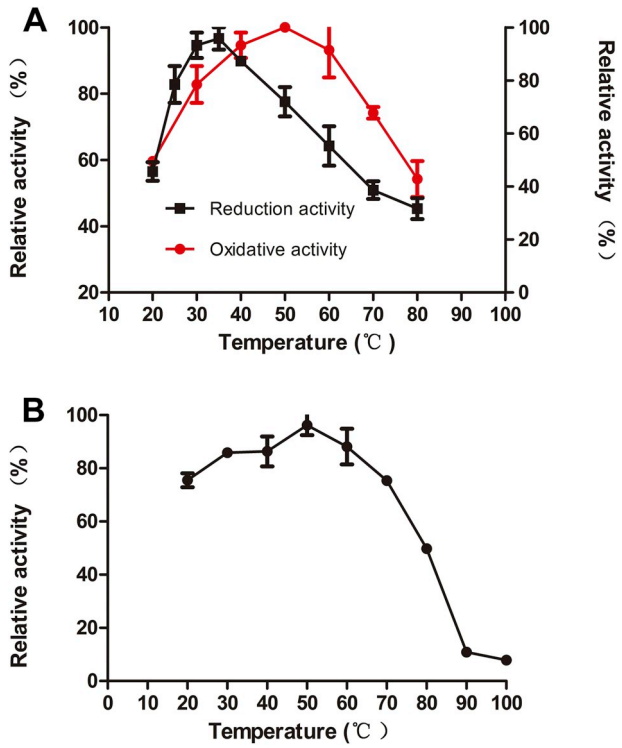

Fig. 5. Effects of temperature on the *Bt*BDH activity and stability. **A**. The effect of temperature on oxidation reaction and reduction reaction. **B.** The temperature stability of *Bt*BDH for oxidation of (2R,3R) -butanediol. The reductase activities were measured with substrate concentrations of 10 mM and 300 μM NAD(H) in PBS (50 mM, pH 7.5), the oxidase activity was measured in Gly/NaOH buffer (50 mM, pH 10.0). Data are represented in the means of triplicate experiments, and error bars are shown by the standard deviation.

Table 2
Effects of some compounds and metal ions on the activity of *Bt*BDH.

Compounds	Concentrations (mM)	Relative activity (%)
Control	0	100
KCl	1	150 ± 15.52
NaCl	1	88 ± 3.58
$CoCl_2$	1	111 ± 8.60
$MgCl_2$	1	106 ± 2.34
Ni_2SO_4	1	71 ± 2.85
LiCl	1	95 ± 8.98
$CaCl_2$	1	106 ± 6.16
$MnCl_2$	1	169 ± 13.36
$MnSO_4$	1	223 ± 12.82
$ZnCl_2$	1	92 ± 14.68
$FeCl_3$	1	105 ± 5.13
Triton X-100	10	90 ± 9.76
DTT	10	108 ± 12.00
DMSO	10	96 ± 6.15
EDTA	10	9 ± 0.26
SDS	10	9 ± 0.26
Tween80	10	110 ± 5.28

Values given are average of three replications. Data are the mean ± SD.

reduction activity was obtained at pH 7.5 and 35 °C. Besides, it displayed remarkable stability over a wide pH range (6–10) and temperatures up to 70 °C. *Bt*BDH showed a good stability after storage for 3-month at 4 °C, and its excellent stability guarantees its potential industrial applications. Moreover, the enzymatic activity is elevated by K^+, Co^{2+} and Mn^{2+} and is specifically regulated by Zn^{2+}. In contrast, EDTA inhibits the enzyme activity, indicating that it is a metal-dependent dehydrogenase. The excellent oxidative activity of *Bt*BDH makes it a promising candidate enzyme in the production of acetoin.

Table 3
The effects of Zn^{2+} on the activity of butanediol dehydrogenases.

$ZnCl_2$ (mM)	Relative activity (%)
Control	100 ± 8.53
0.1	117 ± 6.59
0.5	96 ± 6.21
1	86 ± 7.94
5	86 ± 10.92
10	86 ± 2.57

Values given are average of three replications. Data are the mean ± SD.

Declaration of competing interest

The authors declare that there is no conflict of interest regarding the publication of this paper.

Acknowledgements

This work was supported by Innovation Fund of Dalian Institute of Chemical Physics (DICP ZZBS201704; DICP BioChE-X201801), National Natural Science Foundation of China (31670803) and the Natural Science Foundation of Liaoning Province, China (20170540027).

References

Banfield, M.J., Salvucci, M.E., Baker, E.N., Smith, C.A., 2001. Crystal structure of the NADP(H)-dependent ketose reductase from Bemisia argentifolii at 2.3 A resolution. J. Mol. Biol. 306, 239–250.
Bowyer, A., Mikolajek, H., Stuart, J.W., Wood, S.P., Jamil, F., Rashid, N., Akhtar, M., Cooper, J.B., 2009. Structure and function of the l-threonine dehydrogenase (TkTDH) from the hyperthermophilic archaeon Thermococcus kodakaraensis. J. Struct. Biol. 168, 294–304.
Çelik, A., Aktaş, F., 2013. A new NADH-dependent, zinc containing alcohol dehydrogenase from Bacillus thuringiensis serovar israelensis involved in oxidations of short to medium chain primary alcohols. J. Mol. Catal. B Enzym. 89, 114–121.
Celinska, E., Grajek, W., 2009. Biotechnological production of 2,3-butanediol-Current state and prospects. Biotechnol. Adv. 27, 715–725.
Gao, J., Yang, H.-H., Feng, X.-H., Li, S., Xu, H., 2013. A 2,3-butanediol dehydrogenase from Paenibacillus polymyxa ZJ-9 for mainly producing R,R-2,3-butanediol: purification, characterization and cloning. J. Basic Microbiol. 53, 733–741.
Gonzalez, E., Fernandez, M.R., Larroy, C., Pares, X., Biosca, J.A., 2001. Characterization and functional role of Saccharomyces cerevisiae 2,3-butanediol dehydrogenase. Chem. Biol. Interact. 130, 425–434.
Gonzalez, E., Fernandez, M.R., Larroy, C., Sola, L., Pericas, M.A., Pares, X., Biosca, J.A., 2000. Characterization of a (2R,3R)-2,3-butanediol dehydrogenase as the Saccharomyces cerevisiae YAL060W gene product. Disruption and induction of the gene. J. Biol. Chem. 275, 35876–35885.
Hohn-Bentz, H., Radler, F., 1978. Bacterial 2,3-butanediol dehydrogenases. Arch. Microbiol. 116, 197–203.
Ishikawa, K., Higashi, N., Nakamura, T., Matsuura, T., Nakagawa, A., 2007. The first crystal structure of L-threonine dehydrogenase. J. Mol. Biol. 366, 857–867.
Kochius, S., Paetzold, M., Scholz, A., Merkens, H., Vogel, A., Ansorge-Schumacher, M., Hollmann, F., Schrader, J., Holtmann, D., 2014. Enantioselective enzymatic synthesis of the alpha-hydroxy ketone (R)-acetoin from meso-2,3-butanediol. J. Mol. Catal. B Enzym. 103, 61–66.
Muschallik, L., Molinnus, D., Bongaerts, J., Pohl, M., Wagner, T., Schoening, M.J., Siegert, P., Selmer, T., 2017. (R,R)-Butane-2,3-diol dehydrogenase from Bacillus clausii DSM 8716(T): cloning and expression of the bdhA-gene, and initial characterization of enzyme. J. Biotechnol. 258, 41–50.
Otagiri, M., Kurisu, G., Ui, S., Takusagawa, Y., Ohkuma, M., Kudo, T., Kusunoki, M., 2001. Crystal structure of meso-2,3-butanediol dehydrogenase in a complex with NAD(+) and inhibitor mercaptoethanol at 1.7 angstrom resolution for understanding of chiral substrate recognition mechanisms. J. Biochem. 129, 205–208.
Otagiri, M., Ui, S., Takusagawa, Y., Ohtsuki, T., Kurisu, G., Kusunoki, M., 2010. Structural basis for chiral substrate recognition by two 2,3-butanediol dehydrogenases. FEBS Lett. 584, 219–223.
Raedts, J., Siemerink, M.A.J., Levisson, M., van der Oost, J., Kengen, S.W.M., 2014. Molecular characterization of an NADPH-dependent acetoin reductase/2,3-butanediol dehydrogenase from Clostridium beijerinckii NCIMB 8052. Appl. Environ. Microbiol. 80, 2011–2020.
Robert, X., Gouet, P., 2014. Deciphering key features in protein structures with the new ENDscript server. Nucleic Acids Res. 42, W320–W324.
Smith, P.K., Krohn, R.I., Hermanson, G.T., Mallia, A.K., Gartner, F.H., Provenzano, M.D., Fujimoto, E.K., Goeke, N.M., Olson, B.J., Klenk, D.C., 1985. Measurement of protein using bicinchoninic acid. Anal. Biochem. 150, 76–85.

Suganya, P.S.R., Kalva, S., Saleena, L.M., 2014. Molecular docking and dynamics simulation study on the influence of Zn2+ on the binding modes of aggrecanase with its inhibitors. Comb. Chem. High Throughput Screen. 17, 891–903.
Tan, Y., Liu, Z.-Y., Liu, Z., Li, F.-L., 2015. Characterization of an acetoin reductase/2,3-butanediol dehydrogenase from Clostridium ljungdahlii DSM 13528. Enzym. Microb. Technol. 79–80, 1–7.
Tani, A., Sakai, Y., Ishige, T., Kato, N., 2000. Thermostable NADP(+)-dependent medium-chain alcohol dehydrogenase from Acinetobacter sp. strain M-1: purification and characterization and gene expression in Escherichia coli. Appl. Environ. Microbiol. 66, 5231–5235.
Thirumoorthy, N., Manisenthil Kumar, K.T., Shyam Sundar, A., Panayappan, L., Chatterjee, M., 2007. Metallothionein: an overview. World J. Gastroenterol. 13, 993–996.
Uthoff, S., Steinbuchel, A., 2012. Purification and characterization of an NAD+-dependent XylB-like aryl alcohol dehydrogenase identified in Acinetobacter baylyi ADP1. Appl. Environ. Microbiol. 78, 8743–8752.
Xiao, Z., Lu, J.R., 2014. Generation of acetoin and its derivatives in foods. J. Agric. Food Chem. 62, 6487–6497.
Xie, N.-Z., Chen, X.-R., Wang, Q.-Y., Chen, D., Du, Q.-S., Zhou, G.-P., Huang, R.-B., 2017. Microbial routes to (2R, 3r)-2,3-butanediol: recent advances and future prospects. Curr. Top. Med. Chem. 17, 2433–2439.
Xie, N.-Z., Shi, Y.-M., Li, J.-X., Huang, Y.-Y., Du, Q.-S., Huang, R.-B., 2017. Research progress in biological production of chiral acetoin. Guangxi Sci. 24, 33–39.
Xu, G.-C., Bian, Y.-Q., Han, R.-Z., Dong, J.-J., Ni, Y., 2016. Cloning, expression, and characterization of budC gene encoding meso-2,3-butanediol dehydrogenase from Bacillus licheniformis. Appl. Biochem. Biotechnol. 178, 604–617.
Yennawar, H., Moller, M., Gillilan, R., Yennawar, N., 2011. X-ray crystal structure and small-angle X-ray scattering of sheep liver sorbitol dehydrogenase. Acta Crystallogr. D Biol. Crystallogr. 67, 440–446.
Ying, X., Ma, K., 2011. Characterization of a zinc-containing alcohol dehydrogenase with stereoselectivity from the hyperthermophilic archaeon Thermococcus guaymasensis. J. Bacteriol. 193, 3009–3019.
Ying, X., Wang, Y., Xiong, B., Wu, T., Xie, L., Yu, M., Wang, Z., 2014. Characterization of an allylic/benzyl alcohol dehydrogenase from Yokenella sp. strain WZY002, an organism potentially useful for the synthesis of alpha,beta-unsaturated alcohols from allylic aldehydes and ketones. Appl. Environ. Microbiol. 80, 2399–2409.
Yu, B., Sun, J., Bommareddy, R.R., Song, L., Zeng, A.-P., 2011. Novel (2R,3R)-2,3-butanediol dehydrogenase from potential industrial strain paenibacillus polymyxa ATCC 12321. Appl. Environ. Microbiol. 77, 4230–4233.
Yu, M., Huang, M., Song, Q., Shao, J., Ying, X., 2015. Characterization of a (2R,3R)-2,3-butanediol dehydrogenase from Rhodococcus erythropolis WZ010. Molecules 20, 7156–7173.
Zhang, G.L., Wang, C.W., Li, C., 2012. Cloning, expression and characterization of meso-2,3-butanediol dehydrogenase from Klebsiella pneumoniae. Biotechnol. Lett. 34, 1519–1523.
Zhang, H., Zhao, Y., Cao, H., Mou, G., Yin, H., 2015. Expression and characterization of a lytic polysaccharide monooxygenase from Bacillus thuringiensis. Int. J. Biol. Macromol. 79, 72–75.
Zhao, X., Zhang, X., Rao, Z., Bao, T., Li, X., Xu, M., Yang, T., Yang, S., 2015. Identification and characterization of a novel 2,3-butanediol dehydrogenase/acetoin reductase from Corynebacterium-crenatum SYPA5-5. Lett. Appl. Microbiol. 61, 573–579.